1-30-2010

# Neuronal elasticity as measured by atomic force microscopy

Mirela Mustata
*Purdue University - Main Campus*

Ken Ritchie
*Purdue University - Main Campus*, kpritchie@purdue.edu

Helen A. McNally
*Purdue University - Main Campus*, mcnallyh@purdue.edu



Mustata, Mirela; Ritchie, Ken; and McNally, Helen A., "Neuronal elasticity as measured by atomic force microscopy" (2010). *Birck and NCN Publications.* Paper 676.
http://dx.doi.org/10.1016/j.jneumeth.2009.10.021

Journal of Neuroscience Methods 186 (2010) 35–41

Contents lists available at ScienceDirect

Journal of Neuroscience Methods

journal homepage: www.elsevier.com/locate/jneumeth

# Neuronal elasticity as measured by atomic force microscopy

Mirela Mustata[a,c], Ken Ritchie[a], Helen A. McNally[b,c,*]

[a] Department of Physics, Purdue University, West Lafayette, IN, 47906, United States
[b] Department of Electrical and Computer Engineering Technology, Purdue University, West Lafayette, IN, 47906, United States
[c] Bindley Biosciences Center and Birck Nanotechnology Center, Purdue University, West Lafayette, IN, 47906, United States

ARTICLE INFO

*Article history:*
Received 29 December 2008
Received in revised form 28 October 2009
Accepted 29 October 2009

*Keywords:*
Atomic force microscopy
Membrane elasticity
Acrolein

ABSTRACT

A cell's form and function is determined to a great extent by its cellular membrane and the underlying cytoskeleton. Understanding changes in the cellular membrane and cytoskeleton can provide insight into aging and disease of the cell. The atomic force microscope (AFM) allows unparalled resolution for the imaging of these cellular components and the ability to probe their mechanical properties. This report describes our progress toward the use of AFM as a tool in neuroscience applications. Elasticity measurements are reported on living chick embryo dorsal root ganglion and sympathetic neurons in vitro. The neuronal cellular body and growth cones regions are examined for variations in cellular maturity. In addition, cellular changes due to exposure to various environmental conditions and neurotoxins are investigated. This report includes data obtained on different AFM systems, using various AFM techniques and thus also provides knowledge of AFM instruments and methodology.



## 1. Introduction

Since its inception, researchers have been using the atomic force microscope (Binnig et al., 1986) to investigate cellular form and function (Morris et al., 1999; Haydon et al., 1996; Jena and Hoerber, 2006; Parpura et al., 1993; Nagao and Dvorak, 1998; Kumar and Hoh, 2001; Kacher et al., 2000; Diaspro and Rolandi, 1997; Haberle et al., 1992), biomolecules (Engel et al., 1999; Fotiadis et al., 2002; Hansma, 1999; Chen and Hansma, 2000), and to characterize surfaces for biologic attachment (Muller et al., 1997; Wojcikiewicz et al., 2004; Guimard et al., 2007). The use of AFM significantly increased on soft biological samples when the tapping mode was developed (Hansma et al., 1994) which increased resolution and reduced sample damage. The AFM provides unparalled three-dimensional imaging of living cells in physiologically relevant conditions. Additionally, the AFM is capable of manipulating and interacting with the sample providing additional physical measurements such as elasticity (Radmacher, 1997), binding constants (Lee et al., 1994), and imaging of underlying cellular organelles (Vinckier et al., 1995). A wide spectrum of cells has been studied using AFM technology to include renal cells (Henderson and Oberleithner, 2000), bone (Lehenkari et al., 2000a,b) and neural cells (Grzywa et al., 2006). We have studied living primary neural cells of chick embryos (McNally et al., 2005) and used the AFM to cause irreparable damages to neural cells (McNally and Borgens, 2004) in hopes to better understand the mechanisms of nerve damage and repair.

The elasticity of a cell provides important information toward the health and function of the cell (Costa, 2003). This has been shown in greatest detail in studies of normal and diseased red blood cells (Mohandas and Evans, 1994). Cellular elasticity measurements have been made using techniques such as micropipette aspiration (Evans et al., 1984), the biomembrane force probe (Heinrich et al., 2001), optical tweezers (Dai and Sheetz, 1995; Sleep et al., 1999), magnetic tweezers (Bausch et al., 1999) and others. The AFM has been used to measure elasticity of many cellular types (Radmacher, 1997; Mathur et al., 2001). However, very few experiments have involved neurons (Chumakova et al., 2000; Grzywa et al., 2006; Lal et al., 1995; Tojima et al., 2000) particularly in the living state (McNally and Borgens, 2004; McNally et al., 2005).

Elasticity values can be obtained using the AFM by performing force curve measurements over an extended area (sometimes referred to as force volume (Digital Instruments, 1996)). Fig. 1 shows a typical force curve in contact mode in air on a hard surface. Initially (points 1–2) the cantilever deflection is zero as the tip is brought close to the surface until it begins to deflect downward due to local attractive forces between the tip and surface. This is generally due to a water layer on the sample surface and is termed the "snap to" section. The cantilever then begins to deflect up as the surface and tip come into contact and it continues in a linear fashion as the hard surface continues to push further upward on the tip (points 2–3). The retraction is also very linear as the surface begins to retract away from the tip (points 3–4). It continues to pull the tip down even past the zero deflection point due to adhesion which

* Corresponding author at: Knoy Hall of Technology, 401 North Grant Street, West Lafayette, IN, 47907-2021, United States. Tel.: +1 765 494 7491; fax: +1 765 496 1354.
*E-mail address:* mcnallyh@purdue.edu (H.A. McNally).

0165-0270/$ – see front matter © 2009 Elsevier B.V. All rights reserved.
doi:10.1016/j.jneumeth.2009.10.021

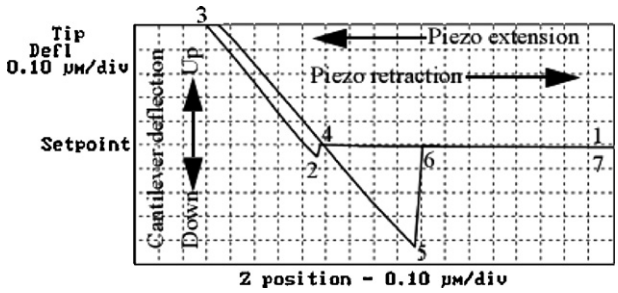


**Fig. 1.** AFM force curve in contact mode (Digital Instruments, 1996).

may occur between the tip and surface (points 4–5). Adhesion can be caused by the water layer or other attractive forces between the tip and sample (i.e. electrostatic forces). Eventually the adhesive contact will be ruptured due to the stiffness of the cantilever and the tip will pull away from the surface returning to its resting position (points 5–6). Force curves on a soft sample vary mainly in the nonlinear nature of the curve and the hysteresis present while the tip is in contact with the surface during extend and retract. The nonlinear portion of the contact region can be used to determine the approximate elasticity of the soft sample.

This work focuses on elasticity measurements of primary neural cells from chick embryo in the healthy living state, under physiologically relevant conditions, changing environmental conditions, and after exposure to the neurotoxin, acrolein.

## 2. Materials and methods

### 2.1. AFM systems and tips

Three AFM systems were used throughout these experiments. The first system was a Digital Instruments Dimension 3100 SPM using a Nanoscope III controller. The optical capabilities of this system were minimal so an associated Nikon Diaphot was used to identify cells of interest for scanning. In order to record the coordinates of these cells, they were incubated on gridded coverslips glued on the bottom of 35 mm Petri dishes. Imaging only data was collected in tapping mode in an aqueous buffer (neural media) using Veeco DNP tips with nominal spring constants of 0.12 N/m. The second AFM system was a PSIA (Park Systems) XE-120 AFM mounted atop a modified Nikon inverted microscope. Imaging of the neural cells was performed in closed loop contact mode in neural media. Park Systems SICON tips were used with a nominal spring constant of 0.2 N/m. The actual spring constant for each tip used was determined with the manufacturer supplied software resulting in ranges of 0.13–0.24 N/m. Additional experiments were performed using a Veeco Bioscope II. This system completely integrates the AFM with a standard Olympus inverted microscope. Imaging data was collected in tapping mode in neural media using Veeco DNP tips with nominal spring constants of 0.12 N/m. Again the actual spring constants (0.03–0.12 N/m) for each tip used for elasticity measurements were determined using the manufacture supplied software. The force curves recorded with the XE-120 and Bioscope II AFMs were used to extract the elasticity data.

### 2.2. Sample origin, disassociation, and culture

Chick Dorsal Root Ganglia and sympathetic ganglia were dissected from 7.5- to 8-day-old chick embryos by conventional methods (Banker and Goslin, 1998). Individual neurons were obtained from the tissue by dissection, triturating, enzymatic digestion (using trypsin in Puck's medium), and differential centrifugation. Cell density was monitored using a hemocytometer and

**Fig. 2.** Optical micrograph of dorsal root ganglion neural cells from chick embryos. The large box depicts a cell body region which would be studied by AFM. The small box represents a growth cone region for similar AFM investigations.

the desired cell suspension was incubated in 35 mm Petri dishes. For the purposes of this study we attempted to obtain primary cultures on the order of 40,000 cells/35 mm Petri dish plated on a substrate of polyornithine and laminin, and maintained at 37 °C in 5% $CO_2$. Healthy neurons, for example, will attach to the laminin treated substrate and begin to form process within 24 h.

A 2% neuron growth medium (Banker and Goslin, 1998) containing nerve growth factor (NGF), vitamin C, insulin (Sigma Chem. Co. # I-6634), and penicillin/streptomycin (Sigma Chem. Co. # P-0906) was used in these studies. The base medium was prepared from an F-12 Nutrient mixture (Gibco # 21700-075), supplemented with the other adjuncts including conalbumin (Sigma # C-0 880) and horse serum (Gibco # 26050-088) to a final pH of ~7.4, and refrigerated until used. Fig. 2 presents typical cell regions investigated in this study.

### 2.3. Acrolein

The effects on neuronal elasticity following exposure to the neurotoxin acrolein were investigated as our previous studies (Liu-Snyder et al., 2006) have shown significant morphological changes in the cell after just 4 h of exposure. This study found a concentration of 100 μM consistently killed all cells within 12 h. Stock acrolein (10 mM) was made fresh in phosphate-buffered saline (PBS) and maintained in a 4 °C refrigerator. Stock solution was added to the Petri dishes during the experiments to bring the final acrolein concentration to 0.1 mM.

### 2.4. Experimental procedures

Each experiment began with the imaging of a neural cell to identify the cell body and growth cone regions to be investigated. Cells in neural media were removed from the $CO_2$ incubator and placed on the AFM stage. Using the XE-120 (Parks Systems) AFM, imaging was performed in contact mode while with the Dimension and Bioscope II (Veeco) AFM imaging was performed in tapping mode. Either mode has been employed for imaging of cellular systems. This difference was chosen due to the optimizations of the imaging parameters which differ between systems. The Dimension and XE-120 were not equipped with heated stages at the time of the experiments, although they are now available. Thus the experiments on these systems were limited to 2 h which is half the time in which the cells began to show detrimental effects due to temperature changes. Using the Bioscope II, the biological kit (Veeco, Heater

Perfusion Chamber) maintained the temperature by a heated stage and the cells remained viable for a minimum of 8 h.

The AFM systems' (PSIA and Bioscope II) force curve modes were employed to perform the elasticity measurements. Once the cells were identified through AFM imaging, force curves were performed on the regions of interest (cell body and growth cone) as well as calibration force curves were performed on the relatively hard surface where there were no cells found. This relatively hard surface is the polyornithine/laminin (PL) layer which is thin and has minimal effect on the overall force curve. Ten consecutive force curves were performed on each region, the PL layer, the cell body and the growth cone region. In long-term experiments the system would be set up to perform these same force curve measurements every 15 min. Experiments involving acrolein were performed in the same manner. However, to introduce the acrolein into the system a small pipette was used to add the required concentrations into the Petri dish while on the AFM stage without perturbing the cells or the AFM tip. Imaging and elasticity measurements were performed at periodic times to determine the effect of acrolein on the neural cells' growth cone and cell body regions. The health of the cells was visually observed using the optical scope to monitor major morphological changes.

### 2.5. Analysis

Typical force curves for soft materials present three main regions. (1) At large tip-sample distances there are no interaction between the tip and surface so the cantilever deflection does not change. (2) As the tip approaches and begins to indent into the soft sample a nonlinear contact region is revealed. (3) A similar nonlinear region is observed as the tip is withdrawn from the sample, although with a hysteresis as compared to the approaching contact curve. Knowing the properties of the indenter (AFM tip and cantilever), one can predict the elastic properties of the sample from the contact region of the force curve (Butt et al., 2005). Because the force curves recorded for neuronal cell body presented a hysteresis, which in general indicates the viscoelastic behavior of the sample (Lanero et al., 2006), the analysis was done only on the approaching curves. The approach curves were chosen for two reasons. First, the initial response of the cell to AFM probing is captured with the approach data. Secondly, the retract data may be compromised by the loss of contact between the cell and AFM probe as the probe is moved away from the cell. Depending on the geometry of the indenter, the contact region of the sample-tip (cantilever) interaction can be described by the continuum mechanics of elastic contact. We used Sneddon's modified Hertz theory (Sneddon, 1965) for the conical indenter interacting with the elastic half-space,

$$z - z_0 = d - d_0 + \sqrt{\frac{k\pi(1-\nu^2)}{2E_y \cot\alpha}}\sqrt{d-d_0}$$

where $z$ is the position of the piezo, $d$ is the cantilever deflection, $\nu$ is the Poisson's ratio, $k$ is the spring constant of the cantilever, $E$ is Young's modulus and $\alpha$ is the semivertical angle of the indenter. The recorded force curves represent cantilever deflection as a function of the position of the piezo ($z$). Using a Levenberg–Marquadt nonlinear curve fitting algorithm (Originlab Corp. Northampton, MA), the approaching force curves were fit to

$$y = y_0 + \frac{1}{4}\left(\frac{2k\pi(1-\upsilon^2)}{2E_y \cot\alpha} + 4(x-x_0) - 2\sqrt{\frac{k\pi(1-\upsilon^2)}{2E_y \cot\alpha}}\sqrt{\frac{k\pi(1-\upsilon^2)}{2E_y \cot\alpha} + 4(x-x_0)}\right)$$

which represents the solution of Hertz–Sneddon model. The parameters initialized for each curve were Poisson's ratio, the semivertical angle and the spring constant of the cantilever. The Poisson's ratio relates shear stress to compression stress and cannot be determined independently from the Young's modulus in this model. As such, a value of 0.5 was chosen for the Poisson's ratio in this study. For all curves, DNP cantilevers from Veeco were used, with a pyramidal tip with a 35° faces. In this case the semivertical angle used in calculations was 55° or 0.9594 rad, and the cantilevers were calibrated before each measurement, resulting in spring constants from 0.03 to 0.24 N/m. Force curves were performed on cell bodies and growth cones multiple time at a very slow frequency of 0.5 Hz to minimize the viscoelastic effect of the cellular membrane. The next step was to approximate the coordinates of the contact point, $x_0$ and $y_0$. A first iteration of the fitting formula would give better numbers for these parameters. Keeping the Poisson's ration $\nu$, semivertical angle $\alpha$, spring constant $k$, and the coordinates of the contact point $x_0$ and $y_0$ fixed, 100 iterations were performed using the force curve data ($x$ being the piezo position and $y$ being the cantilever deflection) to fit the remaining parameter, the Young's modulus $E_y$ to the experimental curve. The acceptable correlation coefficient was 0.94.

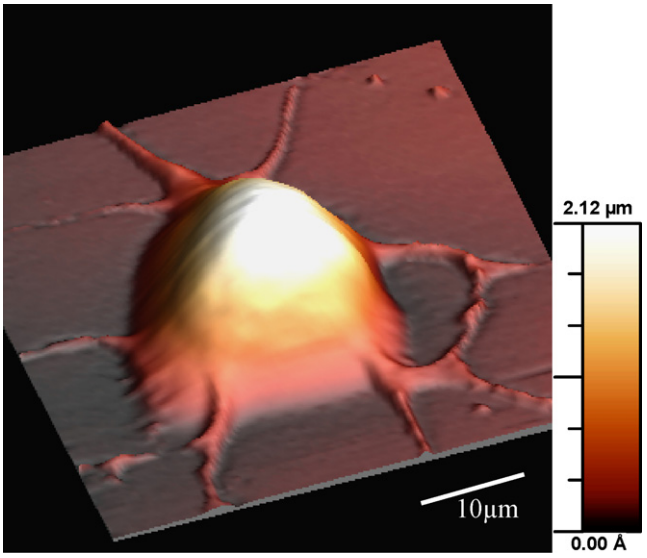


**Fig. 3.** Sympathetic neural cell body imaged in tapping mode with the Bioscope II.

## 3. Results

### 3.1. Imaging

The AFM provides unparalled three-dimensional images of living neurons which have been previously reported (McNally and Borgens, 2004). Vertical projections have been identified as well as the fine fillipodia, lamellipodia and microspikes associated with the developing growth cone. Fig. 3 shows an AFM image of the cell body region of a sympathetic neural cell taken in tapping mode on the Bioscope II. Contact mode has the advantage of highlighting the underlying cytoskeleton as the AFM tip forces the cellular membrane down around the more stable actin filaments of the cytoskeleton (Pesen and Hoh, 2005). However, this effect alone perturbs the cellular membrane resulting in a convoluted image of the cell. Most researchers perform cellular imaging using tapping mode so the forces of imaging are reduced compared to contact mode and thus providing a more accurate

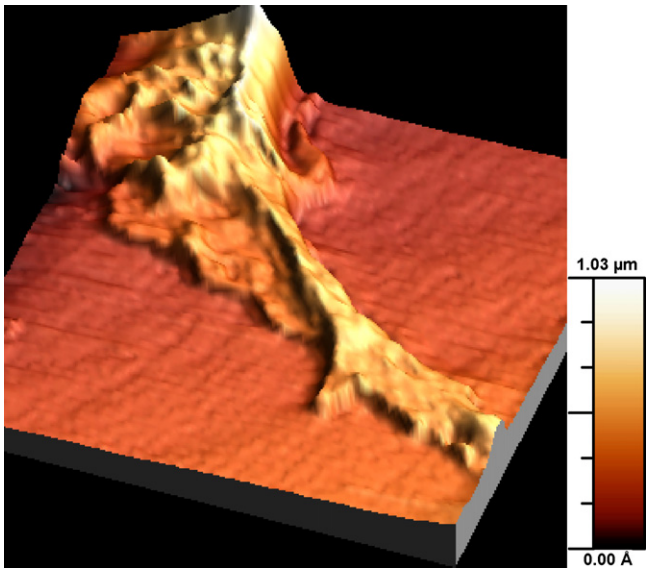


**Fig. 4.** Dorsal root ganglia neural cell growth cone imaged in tapping mode on the Dimension 3100.

image of the cellular topography (Weisenhorn et al., 1989). For this image tapping mode has been used with the highest setpoint possible to minimize the forces exerted on the neural cells.

Fig. 4 shows an AFM image of the growth cone region of DRG neural cell. This image was obtained in tapping mode on the Dimension 3100. The fillipodia, lamellipodia, and microspikes of the developing growth cone are apparent. As well, the growth cone has a curious ridge-like back bone which has been previously reported (McNally and Borgens, 2004) and confirmed with confocal microscopy (McNally et al., 2005).

AFM imaging of cell bodies and growth cone regions such as these were made over extended periods of time with no detrimental effect to the cell. To confirm the AFM tip was not affecting the cell, imaging was performed for over an hour and then the cells were placed back into the incubator. A solution of trypan blue was applied 24 h later to determine if the cells were viable. In each case the cells imaged maintained the same percentage of viability as those which had not been imaged. Imaging was also performed over a number of hours to determine the length of time the cells would remain viable while on the AFM stage. Without the controlled environment of the heated stage, the neural cells began to show negative effects after 4 h. At this time the growth cones would begin to retract, the cell body would begin to round, and adhesion point would begin to release from the surface. Using the heated stage on the Bioscope II, cells would remain healthy under continuous imaging for 8 h. Longer experiments were not performed on these cells.

Neural cells exposed to the neurotoxin, acrolein, demonstrated detrimental effects in a much shorter time frame as shown in Fig. 5. Initially a healthy cell is imaged showing the cell body and extending dendrites (panel a). The microspikes, lamellipodia and fillipodia are all evident and the cell is securely attached to the substrate. After 15 min of exposure to acrolein, the cell morphology begins to change (panel b); the lower dendrite begins to move toward the left of the frame while the lamellipodia on the right become discontinuous. 45 min later the cell body as moved to the left and the lamellipoda on the top right is retracting (panel c). After 75 min of exposure to acrolein, the cell body has moved to the left and nearly released from the surface (panel d). The adhesion point on the bottom right is about to break. Increased time lapsed images were not possible as the cells completely released from the substrate surface, rendering AFM imaging impossible. This was confirmed optically using the associated Nikon Diaphot optical microscope. The experiments involving acrolein were repeated ten times, each resulting in the demise of the exposed cells occurring within ninety minutes. As stated above, cells remained viable showing characteristic morphologies of healthy cells for a minimum of 4 h without using a heated stage and up to 8 h with the heated stage.

### 3.2. Elasticity measurements

Initially force curves were performed on the neural cell body and growth cone region to measure the membrane elasticity in these regions which was anticipated to identify differences in the maturity of the cellular membrane. Fig. 6 presents typical data taken on the (a) cell body and (b) growth cone regions. The polyornithine/laminin layer is thin and results in a force curve typical of a hard surface as seen in Fig. 1. The "snap to" portion of the curve is not seen as this effect is not realized when operating in fluids. On the cell body, the contact region is nonlinear and show hysteresis between the extension and retraction portions of the curve. The nonlinearity is expected as the cell body is compressible and thus the AFM tip is not deflected as it would be with a hard surface. The hysteresis of the nonlinear portion is a result of the viscoelasticity of the cell body as the cell resists the forces of the tip differently during the extension as compared to the tip retraction. The entire range of extension and retraction is nonlinear as the cell body is much thicker than the range of motion of the tip, in this case 2 μm. In the case of the growth cone region, it has been shown to be typically 200 nm thick (McNally and Borgens, 2004). The applicability of Sneddon's approximation to the growth cone region is not valid as the minimal thickness of the sample must be greater than 300 nm in order to assume a semi-infinite geometry (Domke and Radmacher, 1998). To reduce this effect we only fitted the nonlinear portion of the force curve where the tip/sample interaction was less than the thickness of a typical growth cone. As expected, our results (data not shown) were inconsistent, confirming the work of Domke and Radmacher in 1998. The growth cone region also shows less hysteresis. This is expected as the growth cone region is not as mature as the

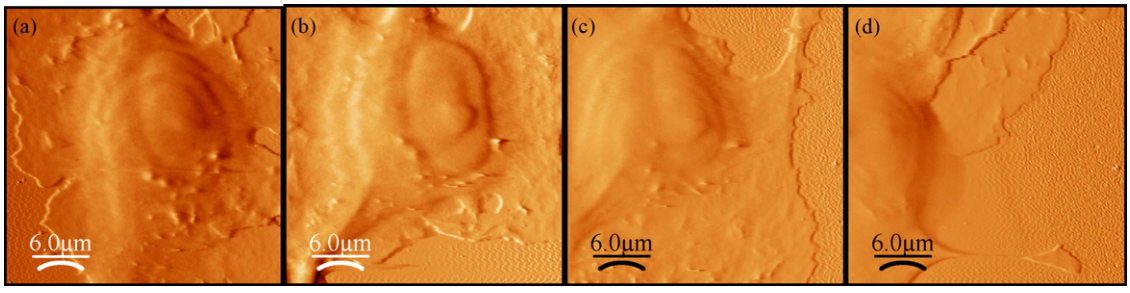


**Fig. 5.** Time lapse amplitude images of DRG neural cells exposed to acrolein, (a) 5 min prior to acrolein exposure, (b) 15 min after exposure, (c) 45 min after exposure, and (d) 75 min after exposure.

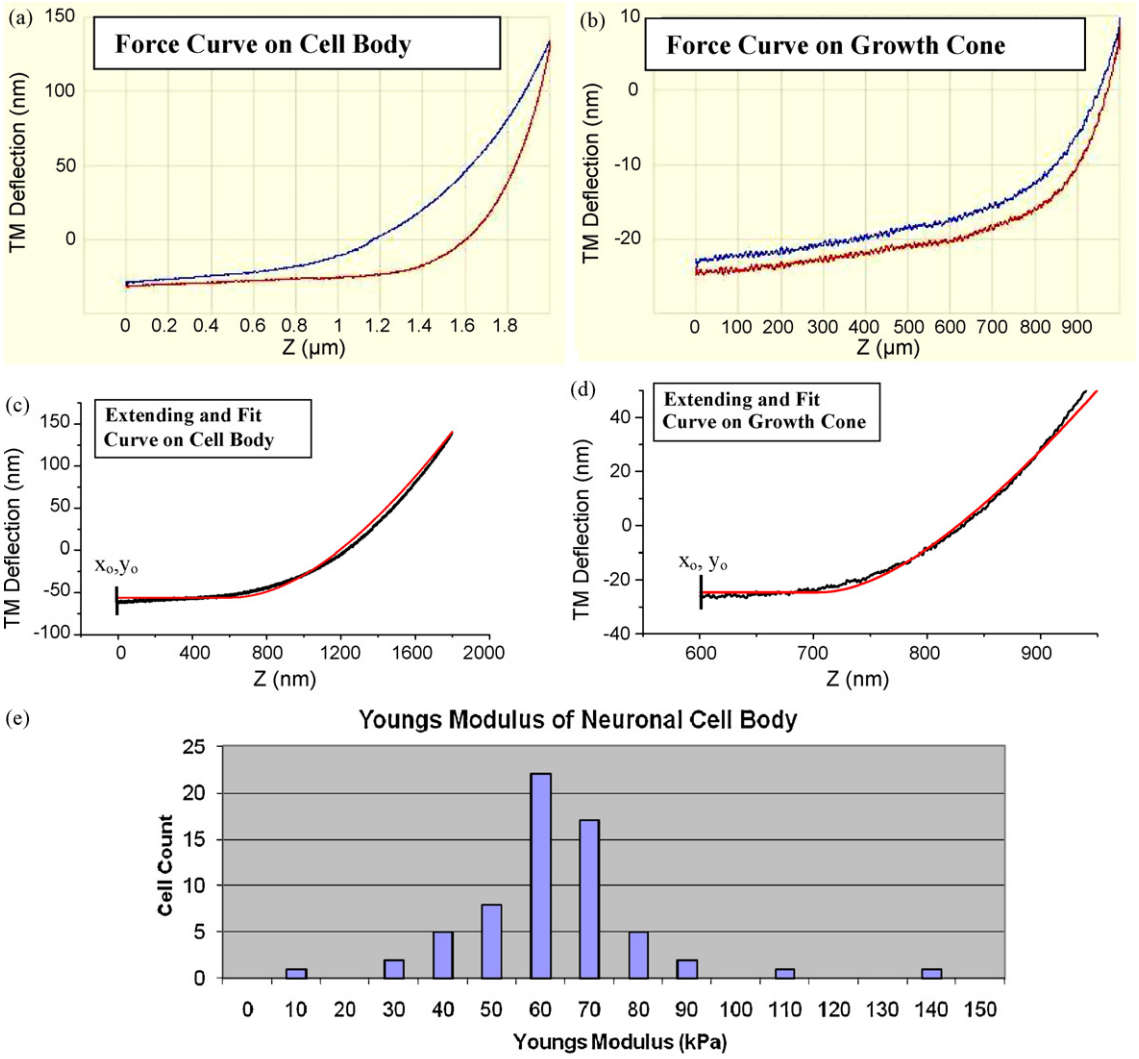


**Fig. 6.** Force curves typical of (a) neural cell body and (b) growth cone region. The red trace represents the extending portion of the force cure while the blue curve represents the retraction portion. (c) and (d) panels show the extending portion of the curves in black and the fitted curve in red for the cell body and growth cone regions, respectively. (e) Illustrates the average elasticity data for cell body regions of healthy neural cells.

cell body and thus does not resist the force of the AFM tip as well. Panels (c) and (d) show the fitted curves with the extension curve for the cell body and growth cone regions, respectively. Quantitative data on over 50 cell bodies are presented in panel (e). Average Young's moduli of 60 kPa are typical of those found on many other types of cells (Radmacher, 1997). Modulus of significantly higher or lower values can be expected due to the heterogeneity of cells. While the AFM probe contacts the cell at designated points, it is not known if the underlying structure of the cell consists of the cytoskeleton, organelles, or vacuoles to name a few. Each of these substructures affect the elasticity measurements differently.

In order to better understand the long-term effects of AFM probing and environmental conditions on the viability of the neurons, extended experiments were conducted on the Bioscope II using the heated stage. The heated stage was able to keep the fluid in the Petri dish at an average of 35 °C with the acoustic enclosure closed. The cells were imaged to identify the cell body and/or growth cone region to be measured. Force curves were then performed every 15 min over an 8-h period (data not shown). Data on the cell bodies was consistent with an average elasticity similar to those shown previously. However, on the growth cone regions the data fluctuated greatly as would be expected as the growth cone developed and changed positions. Similar experiments were performed without the heated stage to determine the effect on the viability of the neural cells. This data was consistent with those obtained on the XE-120 which did not have the heated stage. The neural cell body presented an average elasticity of 60 kPa for typically 4 h, after which the elasticity was reduced indicating degradation of the cell body and ultimately the cell body released from the surface within 6 h. In the case of the growth cone regions, elasticity changed much quicker, usually within 30 min elasticity measurements were typical of force curves on the PL substrate. These results can be explained by the initial degradation of the growth cone which would occur much earlier than the cell body and then the retraction of the growth back into the cell body leaving the PL layer only to be probed. This process was confirmed using the optics associated with both the Bioscope II and the XE-120 AFMs.

Knowing the timeframe for the viability of neural cells on the AFM heated stage, experiments were performed to access the effect of the neurotoxin, acrolein. Cells were again imaged to identify the cell body and/or growth cone regions and then force curves were performed on the cells prior to exposure to acrolein. Once a baseline was established, the acrolein solution was introduced to the Petri dish and force curves were performed every 10 min. Force curves were performed on the cell body and growth cone regions using

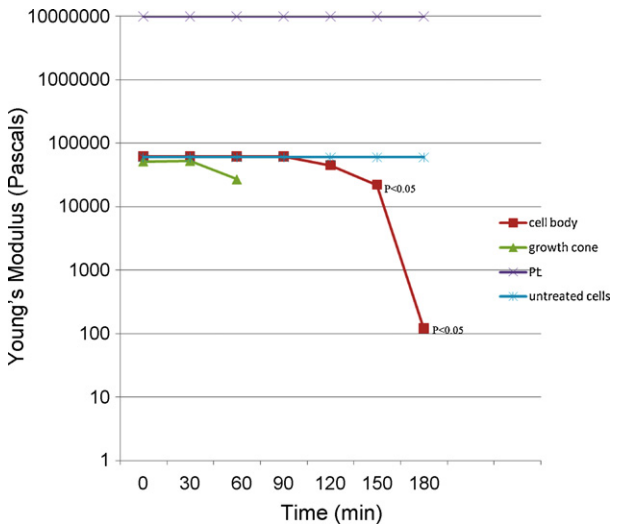


**Fig. 7.** Elasticity measurements of the neuronal cell body and growth cone exposed to acrolein. $T=0$ indicates the time of introduction of acrolein. Elasticity measurements of healthy neural cells and the polyornithine/laminin layer are also shown as a reference to the reader. Error bars are not apparent due to the log scale. Error bars are PL ±1%, untreated ±3%, cell body ±3.4%, 3.1%, 3.5%, 4.2%, 6.2%, 5.9%, 6.3%, growth cone ±5%, 6.8%, 9.2%.

twenty fresh samples (ten for the cell body and ten for the growth cone). The elasticity of the cell body remained consistent for 1 h and then began to reduce, indicating loss of rigidity in the cellular cytoskeleton which supports the cellular membrane. This decrease in elasticity would continue until a sharp increase toward a Young's modulus of 10 MPa. As shown in Fig. 5, the cellular body would ultimately release from the substrate, making elasticity measurements meaningless. The measurement of elasticity is not possible if the cell is not securely attached to the sample substrate. Over time, many cells would release from the surface and/or attach to the AFM tip, in addition to degrading which would allow the tip to interact with the surface thus affecting the elasticity measurements. Therefore, measurements of 10 MPa or more were considered to be influenced by the substrate and were not used in the analysis of this data. A similar effect was seen in the growth cone regions but in a shorter timeframe. The effects of the acrolein were seen within 30 min with the elasticity first reducing but ultimately the retraction of the neuronal growth cone would leave only the PL layer to be probed. This resulted in data in the range of 10 MPa and again this data was not used during the analysis. Release of the cell bodies from the surface and retraction of the growth cones from the region of measurements were verified with the optical capabilities of the Bioscope II and XE-120 AFM systems. Fig. 7 presents the average elasticity data for the cell body and growth cone regions with respect to time. The Young's modulus of the PL layer (and Petri dish) is shown at 10 MPa and the average elasticity of healthy cells is shown.

## 4. Discussion

AFM techniques have been applied to neural cells providing three-dimensional imaging of living cells and measurements of the membrane elasticity. Three-dimensional imaging of living cellular body and growth cone regions are provided as well as temporal images of the cellular response to neurotoxins. The AFM provides morphology images of living cells with resolutions unparalleled by any other imaging modality. Both regions were also investigated to determine the viability of cells following AFM probing and time out of the incubator on heated and unheated stages using various AFM systems. These test show the AFM probing does not affect the health of the cell on a heated stage and provide time limits for experiments performed on nonheated stages. Measurements of the cellular body elasticity are determined, although the current technique does not allow for a consistent measurement in the growth cone region. Specifically, AFM elasticity measurements of cellular regions less than 300 nm thick are affected by the underlying substrate. An alternative method for these regions must be found. Cells morphology and elasticity were also studied following the application of the neurotoxin, acrolein. Cellular responses on the order of 15 min were detected in morphology and elasticity. Thus AFM imaging and elasticity measurements can be used to detect cellular changes due to environmental conditions and neurotoxins. Our results show the AFM to be a versatile tool for neuroscience application.

Three AFM systems were used in this research and each provided unique benefits and challenges to live cell experiments. The Veeco Dimension 3100 is easy to learn, robust and extremely stable, although it is not optimized for live cell imaging. The optical capabilities are minimal which requires additional steps to identify the cells of interest and locate them on the AFM stage. The configuration of our Dimension 3100 included a Nanoscope III controller which does not allow for closed loop control. This is why only imaging data was obtained on this system and not elasticity measurements. Although not required, closed loop control increases the reliability of elasticity measurements as the tip position can be identified more accurately. Closed loop control is now available with a different controllers as well as better live cell capabilities such as a heated stage and media flow through the Petri dish. The PSIA XE-120 was designed for biological applications. It is integrated into a modified Nikon inverted microscope. This allows for bottom view optics. The system has very nice control of approach toward the sample and it is very robust making it an excellent system for novice users. At the time of these experiments a heated stage and flow through capabilities were not available; however those capabilities are now options for purchase through PSIA. The Veeco Bioscope II completely integrates the AFM into a standard Olympus (and other manufacturers) microscope allowing full optical capabilities such as bight field, phase contrast and integration with confocal and multi photon microscopy. It uses an infrared laser for AFM detection to eliminate interference with fluorescence measurements. The scope includes a full biological kit with flow through and heated stage. AFM systems such as the PSIA XE-120 and Bioscope II designed specifically for biological applications provide the best alternative for live cell AFM imaging combined with optical techniques; however they lose some stability when mounted on top of optical microscopes. AFM systems used for elasticity measurements should employ closed loop control to maintain accurate vertical positioning. Of the systems utilized in this research, the Bioscope II provided the best system configuration and options for live cell imaging and elasticity measurements. However, many manufacturers are currently developing systems for these purposes or optimizing the current configurations to meet the high interest of the biological community in these techniques. Researchers should determine their specific experimental requirements and perform a thorough product review prior to any purchase.

## Acknowledgements

The authors would like to thank Ms. Judy Grimmer of the Center for Paralysis Research (CPR), Purdue University for her assistance in the cell culture, Dr. Michael Melloch, Department of Electrical and Computer Engineering, Purdue University, Dr. Richard Borgens of the CPR and Veeco Instruments for the use of the Dimension 3100, XE-120 and Bioscope II AFM systems, respectively.

## References


Banker G, Goslin K, editors. Culturing nerve cells. 2nd ed. Massachusetts: The MIT Press; 1998. p. 391.

Bausch AR, Moller W, Sackmann E. Measurement of local viscoelasticity and forces in living cells by magnetic tweezers. Biophys J 1999;76:573–9.

Binnig G, Quate CF, Gerber Ch. Atomic force microscopy. Phys Rev Lett 1986;56(9):930–3.

Butt HJ, Cappella B, Kappl M. Force measurements with the atomic force microscope: technique, interpretation and applications. Surf Sci Rep 2005;59:1–152.

Chen CH, Hansma HG. Basement membrane macromolecules: insights from atomic force microscopy. J Struct Biol 2000;131:44–55.

Chumakova OV, Liopo SA, Chizhik SA, Tayurskaya VV, Gerashchenko LL, Komkov OY. Effects of ethanol and acetaldehyde on isolated nerve ending membranes: study by atomic-forced microscopy. Bull Exp Biol Med 2000(9):921–4.

Costa KD. Single-cell elastography: probing for disease using the atomic force microscope. Dis Markers 2003;19:139–54.

Dai J, Sheetz MP. Mechanical properties of neuronal growth cone membranes studied by tether formation with laser optical tweezers. Biophys J 1995;68:988–96.

Diaspro A, Rolandi R. Scanning force microscopy for imaging biostructures at high-resolution. Eur J Histochem 1997;41:7–16.

Digital Instruments. Support note, NO. 228. Rev E; 1996.

Domke J, Radmacher M. Measuring the elastic properties of thin polymer films with the atomic force microscope. Langmuir 1998;14:3320–5.

Engel A, Lyubchenko Y, Muller D. Atomic force microscopy: a powerful tool to observe biomolecules at work. Trends Cell Biol 1999;9:77–80.

Evans E, Mohandas N, Leung A. Static and dynamic rigidities of normal and sickle erythrocytes. Major influence of cell hemoglobin concentration. J Clin Invest 1984;73(2):477–88.

Fotiadis D, Scheuring S, Muller SA, Engel A, Muller DJ. Imaging and manipulation of biological structures with the AFM. Micron 2002;33:385–97.

Grzywa EL, Lee AC, Lee GU, Suter DM. High resolution analysis of neuronal growth cone morphology by comparative atomic force and optical microscopy. J Neurobiol 2006;55:1529–43.

Guimard N, Gomez N, Schmidt CE. Conducting polymers in biomedical applications. Progr Polym Sci 2007;32:876–92.

Haberle W, Horber JKH, Ohnesorge F, Smith DP, Binnig EG. In situ investigation of single living cells infected by viruses. Ultramicroscopy 1992;42–44:1161–7.

Hansma HG. Varieties of Imaging with scanning probe microscopes. PNAS 1999;96(26):14678–80.

Hansma PK, Cleveland JP, Radmacher M, Walters DA, Hillner PE, Bezanilla M, et al. Tapping mode atomic force microscopy in liquids. Appl Phys Lett 1994;64(13):1738–40.

Haydon PG, Laritius R, Parpura V, Marchese-Ragona SP. Membrane deformation of living glia cells using atomic force microscopy. J Microsc 1996;182:114–20.

Heinrich V, Ritchie K, Mohandas N, Evans E. Elastic thickness compressibility of the Reb cell membrane. Biophys J 2001;81:1452–63.

Henderson RM, Oberleithner H. Pushing, pulling, dragging, and vibrating renal epithelia by using atomic force microscopy. Am J Ren Physiol 2000;278: F689–701.

Jena BP, Hoerber JK, editors. Force microscopy applications in biology and medicine. John Wiley and Son's; 2006.

Kacher CM, Weiss IM, Stewart RJ, Schimdt CF, Hansma PK, Radmacher M, et al. Imaging microtubules and kinesin decorated microtubules using tapping mode atomic force microscopy in fluids. Eur Biophys J 2000;28:611–20.

Kumar S, Hoh J. Probing the machinery of intracellular trafficking with the atomic force microscope. Traffic 2001;2:746–56.

Lal R, Drake B, Blumberg D, Saner DR, Hansma PK, Feinstein SC. Imaging real-time neurite outgrowth and cytoskeletal reorganization with an atomic force microscope. Am J Physiol 1995;269:C275–85.

Lanero TS, Cavalleri O, Krol S, Rolandi R, Gliozzi A. Mechanical properties of single living cells encapsulated in polyelectrolyte matrixes. J Biotechnol 2006;124:723–31.

Lee GU, Chrisey LA, Colton RJ. Direct measurement of the interaction forces between complementary strands of DNA with atomic force microscopy. Science 1994;266:771–5.

Lehenkari PP, Charras GT, Nesbitt SA, Horton MA. New technologies in scanning probe microscopy for studying molecular interactions in cells. Expert Rev Mol Med 2000a:1–19.

Lehenkari PP, Charras GT, Nykanen A, Horton MA. Adapting atomic force microscopy for cell biology. Ultramicroscopy 2000b;82:289–95.

Liu-Snyder P, McNally HA, Shi R, Borgens RB. Acrolein-mediated mechanisms of neuronal death. J Neurosci Res 2006;84:209–18.

Mathur AB, Collinsworth AM, Reichert WM, Kraus WE, Truskey GA. Endothelial, cardiac muscle and skeletal muscle exhibit different viscous and elastic properties as determined by atomic force microscopy. J Biomech 2001;34:1545–53.

McNally HA, Borgens R. Three-dimensional form in living and dying neurons with atomic force microscopy. J Neurocytol 2004;33(2):251–8.

McNally H, Rajwa B, Sturgis J, Robinson JP. Living neuron morphology imaged with atomic force microscopy and confocal microscopy. J Neurosci Methods 2005;142:177–84.

Mohandas N, Evans E. Mechanical properties of the red cell membrane in relation to molecular structure and genetic defects. Ann Rev Biophys Biomol Struct 1994;23:787–818.

Morris VJ, Kirby AR, Gunning AP. Atomic force microscopy for biologist. Norwich, UK: Imperial College Press; 1999. p. 254.

Muller DJ, Amrein M, Engel A. Absorption of biological molecules to a solid support for scanning probe microscopy. J Struct Biol 1997;119:172–88.

Nagao, Dvorak. An integrated approach to the study of living cells by atomic force microscopy. J Microsc 1998;191(2).

Parpura V, Haydon PG, Sakaguchi DS, Henderson E. Atomic force microscopy and manipulation of living glia cells. J Vac Sci Technol 1993;11(4):773–5.

Pesen D, Hoh J. Modes of remodeling in the cortical cytoskeleton of vascular endothelial cells. FEBS Lett 2005;579:473–6.

Radmacher M. Measuring the elastic properties of biological samples with the AFM. IEEE Eng Med Biol 1997:47–57.

Sleep J, Wilson D, Simmons R, Gratzer W. Elasticity of the red cell membrane and its relation to hemolytic disorders: an optical tweezers study. Biophys J 1999;77:3085–95.

Sneddon IN. The relation between load and penetration in the axisymmetric Boussinesq problem for a punch of arbitrary profile. Int J Eng Sci 1965;3:47–57.

Tojima T, Yamane Y, Takagi H, Takeshita T, Sugiyama T, Haga H, et al. Three-dimensional characterization of interior structures of exocytotic aperatures of nerve cells using atomic force microscopy. Neuroscience 2000;101(2):471–81.

Vinckier A, Heyvaert I, D'Hoore A, McKittrick T, Haesendonck CV, Engleborghs Y, et al. Immobilizing and imaging microtubules by atomic force microscopy. Ultramicroscopy 1995;57:337–43.

Weisenhorn AL, Hansma PK, Albrecht TR, Quate CF. Forces in atomic force microscopy in air and water. Appl Phys Lett 1989;54(26):2651–3.

Wojcikiewicz EP, Zhang X, Moy VT. Force and compliance measurements on living cells using atomic force microscopy (AFM). Biol Proceed Online 2004;6(1):1–9.